Original Article

The Pathology of Aging 129S6/SvEvTac Mice

Veterinary Pathology
2016, Vol. 53(2) 477-492

DOI: 10.1177/0300985815608673
vet.sagepub.com

E. Radaelli[1,2], V. Castiglioni[3], C. Recordati[3], A. Gobbi[4,5], M. Capillo[4,5], A. Invernizzi[6], E. Scanziani[3,7], and F. Marchesi[8]

Abstract

The 129 mouse strain is commonly used for the generation of genetically engineered mice. Genetic drift or accidental contamination during outcrossing has resulted in several 129 substrains. Comprehensive data on spontaneous age-related pathology exist for the 129S4/SvJae substrain, whereas only limited information is available for other 129 substrains. This longitudinal aging study describes the life span and spontaneous lesions of 44 male and 18 female mice of the 129S6/SvEvTac substrain. Median survival time was 778 and 770 days for males and females, respectively. Tumors of lung and Harderian gland were the most common neoplasms in both sexes. Hepatocellular tumors occurred mainly in males. Hematopoietic tumors were observed at low frequency. Suppurative and ulcerative blepharoconjunctivitis was the most common nonneoplastic condition in both sexes. Corynebacteria (primarily *Corynebacterium urealyticum* and *C. pseudodiphtheriticum*) were isolated from animals with blepharoconjunctivitis and in some cases from unaffected mice, although a clear causal association between corynebacterial infections and blepharoconjunctivitis could not be inferred. Polyarteritis occurred only in males and was identified as the most common nonneoplastic contributory cause of death. Eosinophilic crystalline pneumonia occurred in both sexes and was a relevant cause of death or comorbidity. Epithelial hyalinosis at extrapulmonary sites was noted at higher frequency in females. This study contributes important data on the spontaneous age-related pathology of the 129S6/SvEvTac mouse substrain and is a valuable reference for evaluation of the phenotype in genetically engineered mice obtained with this 129 substrain.

Keywords

129 mouse, aging, blepharoconjunctivitis, Harderian gland, hyalinosis, phenotyping

Each inbred laboratory mouse strain exhibits a unique spectrum of naturally occurring lesions that develop progressively with age. Crosses of different strains usually result in variations of the original strain-specific phenotype, which include vanishing, attenuation, or exacerbation of expected lesions or even development of completely new conditions.[20,72] In this context, an accurate definition of strain-specific pathology in those inbred mice that are most frequently used in biomedical research (especially for the generation of genetically engineered mice) is crucial to understand whether a phenotype results from the experimental intervention or rather reflects a naturally occurring entity.[3,54,62] In addition, longitudinal survival studies determining the aging phenotype of inbred strains are particularly important, as they provide a useful reference that enables the selection of the most appropriate genetic background for specific experiments and facilitates the interpretation of clinicopathologic changes that develop in long-term studies.[3,45,72]

Thorough and comprehensive pathologic analysis of inbred strains is important not only for interpreting lesions in the setting of hypothesis-driven research but also for large-scale forward genetic screens that identify novel phenotype-genotype correlations that can be biologically relevant to model-specific aspects of human diseases.[44] This concept holds particularly true for the analysis of aging populations where inbred mice provide a unique experimental tool because of their genetic homogeneity, short life span, and the availability of advanced technologies and comprehensive databases for studying mouse genome and phenome.[62] In this context, there are already several examples where the identification of genetic traits

[1]VIB11 Center for the Biology of Disease, KU Leuven Center for Human Genetics, Leuven, Belgium
[2]InfraMouse, KU Leuven-VIB, Leuven, Belgium
[3]Mouse and Animal Pathology Laboratory, Filarete Foundation, Milan, Italy
[4]COGENTECH SCARL, Milan, Italy
[5]Department of Experimental Oncology, European Institute of Oncology, Milan, Italy
[6]Istituto Zooprofilattico Sperimentale della Lombardia e dell'Emilia Romagna, Sezione di Milano, Milan, Italy
[7]Department of Veterinary Sciences and Public Health, University of Milan, Milan, Italy
[8]School of Veterinary Medicine, College of Medical, Veterinary and Life Sciences, University of Glasgow, Glasgow, Scotland

Supplemental material for this article is available on the *Veterinary Pathology* website at http://vet.sagepub.com/supplemental.

Corresponding Author:
E. Radaelli, VIB11 Center for the Biology of Disease, KU Leuven Center for Human Genetics, Leuven 3000, Belgium.
Email: Enrico.Radaelli@cme.vib-kuleuven.be

underlying specific age-related disorders in inbred mice has been successfully translated into the clinic, proving that similar conditions in humans and mice share common pathomolecular landscapes.[44,52,62,75]

Targeted mutagenesis in mice represents one of the most powerful tools to investigate the genetic basis of diseases. This strategy has made extensive use of the 129 mouse strain as a reference source of embryonic stem cells.[3,53,54,72] Although several mouse lines are grouped under the 129 umbrella, there is a high degree of genetic variability among these substrains as a result of either genetic drift or accidental genetic contamination during outcrossing.[3,53,59,66,67,72] The conundrum associated with this heterogeneous genetic makeup prompted a thorough reclassification of the 129 mouse based on substrain identification and definition in terms of microsatellite markers.[13,59] However, the description of specific phenotypic traits associated with each substrain is far from being completed. In this context, studies that systematically address the aging phenotype (including the full characterization of the pathology of aging) are restricted to few investigations conducted on 129S4/SvJae mice.[3,22,72] From these studies, eosinophilic crystalline pneumonia (ECP) and nephropathy clearly emerged as common nonneoplastic disorders and important causes of death/contributory causes of death (CODs/CCODs).[3,22,72] Pulmonary, hepatic, and Harderian gland tumors were also identified as frequent neoplastic conditions and important CODs/CCODs as well.[3,72]

As comprehensive observations are limited to the 129S4/SvJae mouse, it is currently unclear to what extent the genetic variability existing among the diverse 129 mouse substrains affects the spectrum, latency, frequency, and severity of age-related pathology. While a number of spontaneous disorders may be equally represented over several sublines, major phenotypic differences are expected. Further supporting this notion, distinctive causes of morbidity and/or mortality appear to be more frequently (or exclusively) described in specific 129 substrains while exceedingly rare (or nonexistent) in the 129S4/SvJae mouse. The 129P3/J (129/J) line appears to have an increased proclivity for the development of chronic progressive blepharoconjunctivitis.[60,63] A variety of opportunistic bacteria (eg, *Corynebacterium* spp and *Pasteurella pneumotropica*) have been also associated with this condition, although their actual pathogenetic role is still matter of controversy.[63] In a recent study, bilateral obstructive hydronephrosis resulting from cystinuria and subsequent urolithiasis has been identified as the major cause of death in the 129S2/SvPasCrl mouse. It was then demonstrated that this substrain carries a single pathogenic mutation in the *Slc3a1* gene, which encodes for a subunit of the amino acid transporter present along the brush border of the proximal renal tubules. The resulting loss of function of the transporter is pathogenetically linked to the high frequency of kidney/urinary bladder stones observed in this mouse line. Interestingly, mutation of the ortholog gene is responsible for the same autosomal recessive disorder in humans.[29]

In this work, we report the results of a longitudinal survival study conducted on 44 male and 18 female mice of the 129S6/SvEvTac substrain (http://www.taconic.com/129sve). The investigation aimed to determine several important biological features of this inbred mouse strain, including major clinical manifestations, longevity (life span), spectrum of spontaneous lesions, and contributory causes of morbidity and/or mortality.

Materials and Methods

Animals and Husbandry

A total of 18 female and 44 male 129S6/SvEvTac mice housed in a conventional facility were considered in this study. Animals were individually identified by means of ear tags (Small Animal Ear Tag; National Band & Tag Co, Newport, KY, USA) and multiply housed (up to 5 mice) in open polycarbonate cages (model 1144B; Tecniplast, Buguggiate, Italy) on dust-free wood litter (Lignocel 3?4; Rettenmaier & Sohne, Ellwangen-Holzmühle, Germany). Standard not-autoclaved rodent diet (Teklad 2018 Global 18% Protein Rodent Diet; Harlan Teklad Diets, Madison, WI, USA) and tap water were provided ad libitum. Environmental conditions were controlled with a temperature of 22°C ± 2°C and a 55% ± 10% relative humidity. A 12/12-hour light/dark cycle was applied with the light phase from 7 AM to 7 PM. Mice were included in a health-monitoring program developed in accordance with guidelines of the Federation of European Laboratory Animal Science Associations. The colony tested positive for *Pasteurella pneumotropica*, *Helicobacter hepaticus*, *H. bilis*, *H. rodentium*, *Entamoeba sp*, *Tritrichomonas sp*, *Aspiculuris tetraptera*, *Syphacia obvelata*, and *Myobia musculi*. The colony tested negative for all the other viral and bacterial pathogens listed in the federation's health-monitoring guidelines. Procedures involving animals were performed in accordance with the Italian laws (D.L.vo 116/92 and following additions), which enforced EU 86/609 directive (Council Directive 86/609/EEC of November 24, 1986, on the approximation of laws, regulations, and administrative provisions of the member states regarding the protection of animals used for experimental and other scientific purposes).

Clinical and Pathologic Examination

In this longitudinal survival study, mice were allowed to live for their natural life span, until they showed signs of advanced disease or terminal conditions and were sacrificed with carbon dioxide asphyxiation and submitted for pathologic examination. Complete pathologic examination was also performed on the few mice that died spontaneously. Two levels of clinical examination were routinely conducted on the animals considered in this study: (1) daily visual inspection performed by animal caretakers with the purpose of identifying major behavioral and/or clinical abnormalities; (2) thorough clinical examination performed monthly and before euthanasia by a certified laboratory animal veterinarian, which included a careful observation of mice in their home cage, followed by hands-on physical examination.

Animals euthanized or dying spontaneously were submitted to the Department of Veterinary Sciences and Public Health of

the University of Milan (Milan, Italy) for complete end-of-life pathologic assessment, including necropsy with dissection and histologic examination of the following organs and tissues: brain, heart, kidneys, liver, lung, pancreas, small and large intestine, stomach, spleen, skeletal muscle (quadriceps femoris), skin of the dorsum and from the inguinal region (including mammary gland), a portion of the vertebral column (including spinal cord), sternum, testes with epididymis (males), ovaries and uterine horns (females), trachea, esophagus, and any additional organ/tissue showing macroscopically detectable changes. Both eyes were excised in toto, including Harderian glands, eyelids, and conjunctiva and collected for fixation in Davidson's fluid as previously described.[27] All the other samples were immersion fixed in 10% neutral buffered formalin, routinely processed for paraffin embedding, sectioned at 5 μm, and stained with hematoxylin and eosin for histopathologic examination. Serial sections obtained from representative lesions were also immunostained as detailed in Supplemental Table 1, and Giemsa and Gram stains were performed on selected cases. Sternum and vertebral column were decalcified in a 14% solution of tetrasodium EDTA for 10 days before processing and paraffin embedding.

Upon review and critical consideration of the overall gross and microscopic pathologic findings, the pathologists determined the most likely COD/CCOD for all animals according to criteria outlined in the published literature.[3,26]

Statistical Analysis

Statistical analyses were performed with Graph Pad Prism (version 5.0; GraphPad Software, San Diego, CA, USA). Survival estimates were calculated with Kaplan-Meier survival curves analysis. The Mantel-Cox log-rank test was then used to test for statistically significant differences between sexes. The frequency of neoplastic and nonneoplastic lesions between males and females was compared with Fisher's exact test. Chi-square test and Fisher's exact test were also applied to study the relationship between Harderian gland tumors and the development of blepharoconjunctivitis. $P < .05$ was considered statistically significant.

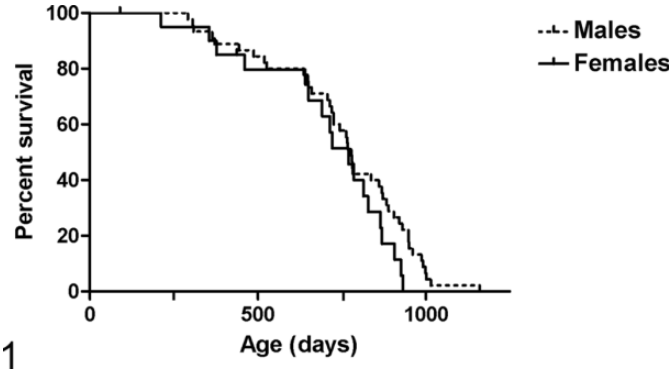

Figure 1. Longitudinal survival study conducted on 129S6/SvEvTac mice. Kaplan-Meier survival curves obtained from 44 males and 18 females.

Table 1. Prevalence of Clinical Abnormalities in Aging Male and Female 129S6/SvEvTac Mice, *n* (%).[a]

Main Categories of Clinical Abnormalities	Males ($n = 44$)	Females ($n = 18$)
Ocular[b]	33 (75)	12 (67)
Perineal/genital region[c]	17 (39)	9 (50)
Skin[d]	18 (41)	9 (50)
Abdominal distension/enlargement	15 (34)	12 (67)
Locomotor impairment[e]	7 (16)	1 (6)
Hyporesponsiveness to stimuli	26 (59)	11 (61)
Slow or labored respiration	16 (36)	9 (50)
Poor body condition/emaciation	23 (52)	10 (56)
Hunched posture	17 (39)	6 (33)
External mass/masses[f]	5 (11)	5 (28)

[a]The data show the number of affected mice per the total number of examined mice (%), based on the last physical examination before death.
[b]Includes eye discharge, eye opacity, crusting, and/or ulceration of the eyelids or exophthalmos.
[c]Includes discharge form orifices, enlargement/swelling or mass, prolapses, or crusting and/or ulceration of the area.
[d]Includes alopecia, scaling, crusting, ulceration, or matted fur.
[e]Includes generalized tremors/convulsions, paraparesis, or vestibular syndrome.
[f]Includes all externally visible masses not affecting the ocular or perineal/genital region.

Results

Longevity (Life Span)

Age range for the entire mouse population considered in this study was 212 to 1160 days, with females ranging between 212 and 932 days and males ranging between 292 and 1160 days. Estimated median survival time was 770 days for the entire mouse population, 770 days for females alone, and 778 days for males alone with no significant sex differences (Fig. 1).

Clinical Findings and End-of-Life Assessment

Daily visual monitoring proved to be an essential measure to prevent early censoring for nonfatal but readily observable lesions (e.g., external masses or lesions affecting eyes, skin, and perineal/genital region) and to prevent loss of pathology data due to unexpected death and postmortem degeneration (autolysis).

Table 1 reports frequencies of the major categories of clinical signs/abnormalities as recorded during the last physical examination before euthanasia or, in a few cases, spontaneous death. The most relevant clinicopathologic correlations encountered in aging 129S6/SvEvTac mice are listed in Supplemental Table 2. Ocular lesions consistent with blepharitis/blepharoconjunctivitis emerged as the most prevalent clinical findings in both sexes (33 of 44 males, 75%; 12 of 18 females, 67%), and abdominal distension was found at the same prevalence in females (12 of 18, 67%). These 2 entities—as well as other categories of nonfatal lesions (including external masses

Table 2. Prevalence of Tumors in Aging Male and Female 129S6/SvEvTac Mice, *n* (%).[a]

Neoplasms	Males ($n = 44$)	Females ($n = 18$)
Brain: ependymoma, malignant	3 (7)	0 (0)
Digestive tract		
Gastric adenocarcinoma	1 (2)	0 (0)
Duodenal adenoma	1 (2)	0 (0)
Endocrine		
Adrenal cortical adenoma	1 (2)	0 (0)
Pituitary adenoma, pars distalis	0 (0)	1 (6)
Harderian gland		
Adenoma, unilateral	11 (25)	1 (6)
Adenoma, bilateral	5 (11)	1 (6)
Adenocarcinoma, unilateral	6 (14)	4 (22)
Adenocarcinoma, bilateral	2 (5)	0 (0)
Hematopoietic system[b]		
Lymphoma	4 (9)	1 (6)
Histiocytic sarcoma	1 (2)	1 (6)
Mast cell sarcoma	1 (2)	0 (0)
Liver		
Adenoma, hepatocellular	9 (21)	3 (17)
Carcinoma, hepatocellular	6 (14)	0 (0)
Lung		
Adenoma	12 (27)	8 (44)
Adenocarcinoma	6 (14)	3 (17)
Reproductive tract		
Endometrial sarcoma	n/a	3 (17)
Endometrial adenocarcinoma	n/a	1 (6)
Uterine hemangioma	n/a	1 (6)
Uterine leiomyoma	n/a	1 (6)
Testicular malignant neoplasm	1 (2)	n/a
Skin		
Mammary adenoma	n/a	1 (6)
Hemangiosarcoma	0 (0)	1 (6)
Squamous cell carcinoma	0 (0)	1 (6)
Total tumors	77	33
Total benign tumors	44	18
Total malignant tumors	33	15
Total metastatic/systemic tumors[b]	7	3

Abbreviation: n/a, not applicable.
[a]Results are reported as number of affected mice per total number of examined mice (%).
[b]These include hematopoietic tumors with multisystemic involvement.

or abnormalities of skin and perineal/genital region)—were always associated with ≥ 1 of the following clinical signs suggestive of imminent death: severe locomotor impairment, hyporesponsiveness to stimuli, slow or labored respiration, poor body condition/emaciation, and hunched posture.

Spectrum of Neoplastic Lesions

The spectrum and frequency of neoplastic lesions are summarized in Table 2. Supplemental Table 3 shows ages at death in the context of the most relevant neoplastic lesions encountered in aging 129S6/SvEvTac mice.

Epithelial neoplasms of the Harderian gland emerged as the predominant tumor type within the study population (30 of 62, 48%), being the most frequent and second-most frequent neoplastic lesion affecting males (24 of 44, 54%) and females (6 of 18, 33%), respectively. Multicentric tumor development with bilateral involvement of both glands was observed in 8 of 30 (27%) cases. Females showed a relatively higher prevalence of malignant tumors (4 of 6, 67%) when compared with males (8 of 24, 33%). Adenocarcinomas were characterized by local invasion of the soft orbital tissues with occasional extension to the skull, brain, and metastatic dissemination to the lungs (Figs. 2–4). Multifocal areas suggestive of myoepithelial differentiation were occasionally observed in both adenomas and adenocarcinomas. However, frequency of this latter observation has not been consistently recorded, and immunohistochemical investigations to confirm and characterize these features were not performed.

Pulmonary epithelial neoplasms (Figs. 5, 6) represented the second-most common tumor type within the study population (29 of 62, 47%), being the most frequent and the second-most frequent neoplastic lesion affecting females (11 of 18, 61%) and males (18 of 44, 41%), respectively. Malignant lesions accounted for about 1 of 3 of the total cases in both sexes. Adenocarcinomas were usually characterized by their large size, invasive nature, intratumoral necrosis, and features of cytoarchitectural atypia (Fig. 6). Multiple lesions were commonly observed, although the frequency of this finding was not consistently recorded.

Hepatocellular tumors also exhibited a relatively high prevalence within the study population (18 of 62, 29%), with males more affected than females (respectively, 15 of 44, 34%; 3 of 18, 17%). In addition, malignant lesions (Fig. 7) accounted for more than one-third of the total cases of hepatocellular tumors in males, whereas only benign lesions were observed in females.

Uterus (together with the Harderian gland) represented the second-most common site of tumor development in females, with 6 of 18 (33%) affected animals. Tumor spectrum in this organ included 3 sarcomas arising from the endometrial stroma (Suppl. Fig. 1) and single cases of endometrial adenocarcinoma, hemangioma, and leiomyoma.

Prevalence of hematopoietic malignancies within the study population was relatively low (8 of 62, 13%). By the time of necropsy, all the hematopoietic tumors had reached an advanced stage of development, showing multiple lesions and/or dissemination to multiple organs and tissues. Five lymphomas were observed (4 in males and 1 in females). Immunohistochemical characterization of the lymphoid neoplasm affecting the female mouse indicated a histiocyte-associated B-cell lymphoma. Two histiocytic sarcomas were observed. One in a male mouse was characterized by a mass at the level of the epididymis, with extensive dissemination to lungs, spleen, liver, kidneys, lymph nodes, and bone marrow (Suppl. Figs. 2–4). The other, in a female, arose in the uterus with local spread to the mesovarium and was characterized by massive necrosis of the affected tissues. Immunohistochemistry for F4/80 and IBA1 confirmed the histiocytic origin of these neoplasms (Suppl.Figs. 3, 4). A single case of mast cell sarcoma

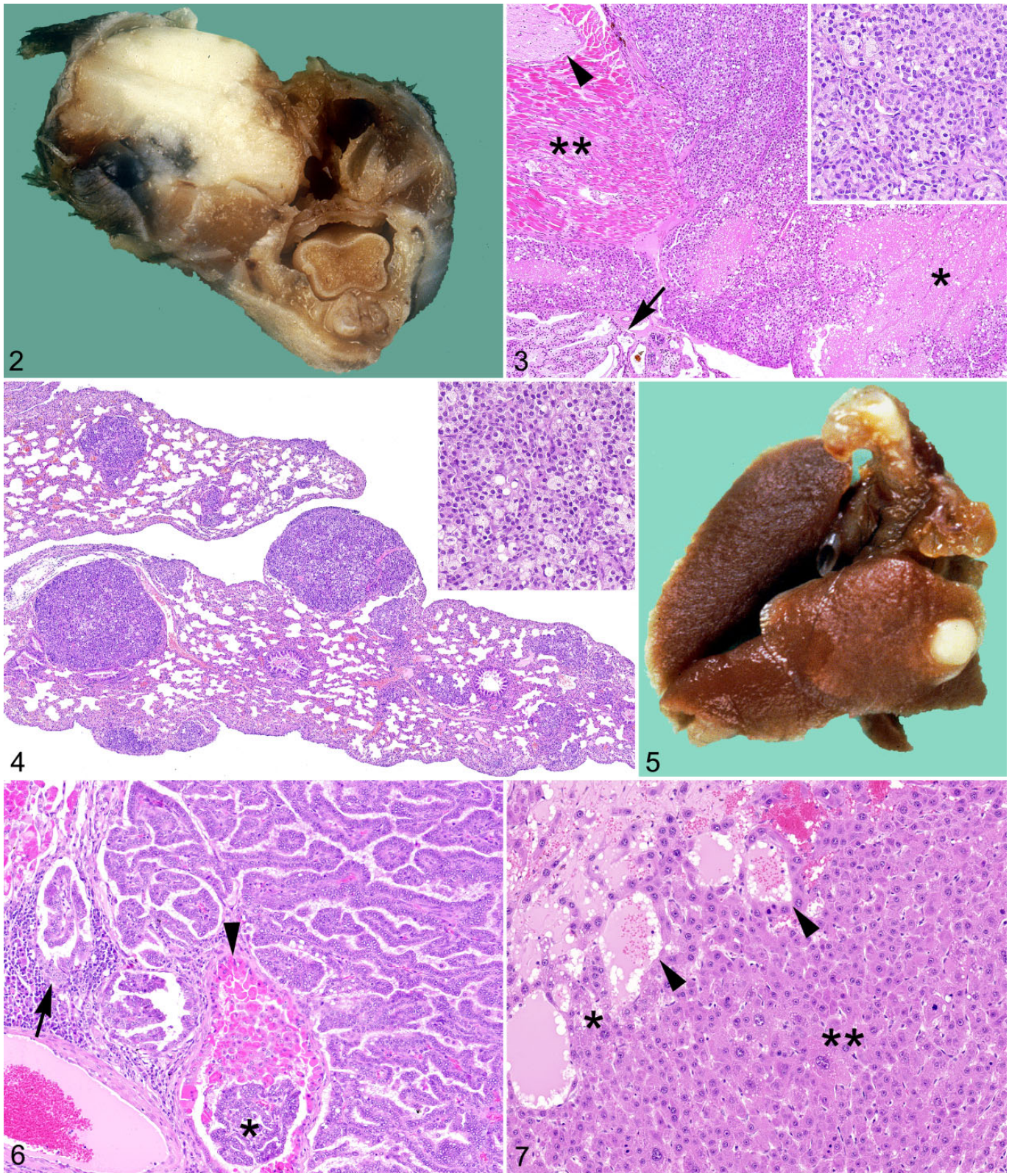

Figures 2–7. Major neoplastic lesions affecting 129S6/SvEvTac mice. **Figure 2.** Unilateral Harderian gland adenocarcinoma, female mouse. The tumor has aggressive growth with local invasion of orbital and periorbital craniofacial structures. **Figure 3.** Unilateral Harderian gland adenocarcinoma, female mouse. The tumor is arranged in solid densely cellular lobules separated by a delicate stroma and accompanied by extensive necrotic areas (asterisk). The neoplastic epithelial cells are cohesive and polygonal with finely vacuolated cytoplasm (inset). Note the residual orbital structures, including Harderian gland (arrow), optic nerve (arrowhead), and extraocular muscles (double asterisk). Hematoxylin and eosin (HE).

was recognized in a male. The tumor displayed a very aggressive nature with a large subcutaneous mass (most likely representing the primary site of development) and massive involvement of lungs, spleen, liver, kidneys, lymph nodes, bone marrow, and skin. Giemsa stain of representative lesions in different organs and tissues demonstrated a prominent granular metachromasia in the cytoplasm of neoplastic cells, confirming the mast cell nature of the tumor (Suppl.Fig. 5).

Other tumors occurred with a low frequency in both sexes. Notably, 3 cases of brain ependymoma were described in males. All tumors showed a clear periventricular distribution and focal continuity with the ependymal lining at the level of the interventricular foramina /third ventricle. Microscopically, neoplastic cells were arranged in pseudorosettes around a prominent vascular network. All ependymomas displayed features of malignancy, including intratumoral necrohemorragic foci and invasion of the surrounding neuroparenchyma. Immunohistochemically, tumors appeared invariably negative for glial fibrillary acidic protein but exhibited diffuse vimentin positivity and wide-spectrum cytokeratin expression in about 20% of tumor cells.

Spectrum of Nonneoplastic Lesions

The spectrum and frequency of nonneoplastic lesions are summarized in Table 3. Supplemental Table 4 shows ages at death in the context of the most relevant nonneoplastic lesions encountered in aging 129S6/SvEvTac mice.

Blepharitis/blepharoconjunctivitis emerged as the most prevalent nonneoplastic condition in males (38 of 42, 90%) and females (15 of 16, 94%). Most affected mice (31 males and 15 females) exhibited bilateral eye involvement. Histologically, lesions were of varying severity. Mild cases showed epidermal acanthosis and hyperkeratosis of the eyelids with crusting of the mucocutaneous junction and minimal infiltrates of inflammatory cells in the subjacent dermis/lamina propria. In more severe cases, eyelids and conjunctival mucosa had suppurative inflammation often accompanied by mucocutaneous erosion/ulceration (Figs. 8, 9). A large proportion of cases (19 males and 11 females) had Gram-positive bacteria in the form of short and occasionally curved rods, frequently in association with the keratin debris accumulating along the eyelid rim (Fig. 9). Clinicopathologic and microbiological investigations were conducted to define the nature and role of Gram-positive rods often described in association with blepharitis/blepharoconjunctivitis (Suppl. Results and Suppl. Table 5). Aging 129S6/SvEvTac mice displayed a high prevalence of blepharitis/blepharoconjunctivitis and Harderian gland tumors, and the occurrence of these lesions was significantly associated ($P = .002$; Suppl. Table 6b). In particular, the presence of Harderian gland tumor proved to be significantly associated with severe blepharoconjunctivitis ($P = .0009$; Suppl. Table 6c).

Accumulation of eosinophilic crystals in the lumen of bronchi/bronchioles and alveoli was the second-most common nonneoplastic lesion in males (30 of 44, 68%) and females (13 of 18, 72%). ECP, formerly known as acidophilic macrophage pneumonia, was also identified as highly frequent nonneoplastic lesion affecting up to 60% of mice in both sexes (Fig. 10). Pulmonary accumulation of eosinophilic crystals and ECP were often accompanied by hyalinosis of bronchial/bronchiolar epithelium. Other organs and tissues exhibiting epithelial hyalinosis were, in order of frequency, glandular mucosa of the stomach (4 of 44 males, 9%; 4 of 18 females, 22%), gall bladder and bile ducts (4 of 44 males, 9%; 4 of 18 females, 22%), transitional epithelium of renal pelvis (2 of 18 females, 11%), and pancreatic ducts (1 of 44 males, 2%; Suppl. Figs. 6–8). Based on these findings, the frequency of epithelial hyalinosis affecting extrapulmonary sites was significantly higher in 129S6/SvEvTac females than males. Last, regardless of the sex of affected animals or type of tissue involved, hyalinosis was consistently accompanied by different degrees of epithelial hyperplasia and inflammatory cell infiltrates with a prominent granulocytic component (Suppl. Figs. 6–8).

Nonneoplastic lesions affecting the cardiovascular system were also highly represented in the aging mouse cohort in this study. Progressive cardiomyopathy was observed in 33 of 62 (53%) mice with a slightly higher frequency in males compared with females. Early myocardial lesions consisted of individual cardiomyocyte degeneration and necrosis. In more severe and chronic cases, this lesion was accompanied by interstitial fibrosis and infiltration of mononuclear inflammatory cells (Suppl. Fig. 9). These changes are consistent with the reported features of murine cardiomyopathy.[12] Polyarteritis was also relatively frequent in males (15 of 44, 34%), whereas females were unaffected. The condition was characterized by a combination of necrotizing and/or proliferative inflammatory changes segmentally affecting the tunica media of small to midsized arteries in several tissues, including heart, pancreas, spleen, kidneys, and gastrointestinal and reproductive tracts (Fig. 11).

The female genital tract represented another major site of nonneoplastic lesion development. In most females (12 of 17, 71%), the uterus presented degenerative and proliferative changes consistent with cystic endometrial hyperplasia (Fig. 12). Angiectasis and thrombosis of myometrial/endometrial blood vessels and suppurative metritis/pyometra were also

Figure 4. Harderian gland carcinoma, pulmonary metastases, female mouse. The pulmonary parenchyma contains disseminated metastatic lesions with the same cytoarchitectural features as the primary tumor (inset). HE. **Figure 5.** Solitary pulmonary carcinoma, female mouse. The tumor forms a well-demarcated whitish solid mass. **Figure 6.** Solitary pulmonary carcinoma, female mouse. The tumor forms a papillary pattern with invasion of the surrounding pulmonary parenchyma (arrow). Note the neoplastic papillae (asterisk) invading and partially replacing a bronchiolar structure characterized by prominent epithelial hyalinosis (arrowhead). HE. **Figure 7.** Hepatocellular carcinoma, male mouse. The tumor has a solid (double asterisk) to trabecular (asterisk) pattern of growth. Dilated sinusoids filled with pale eosinophilic plasma and erythrocytes are visible (arrowheads). HE.

Table 3. Prevalence of Nonneoplastic Lesions in Aging 129S6/SvEvTac Mice, *n* (%).[a]

Organ/Tissue and Lesion	Males	Females
Bones and joints	43	17
Fibro-osseous lesion***	1 (2)	8 (47)
Intervertebral disk degeneration	9 (21)	5 (29)
Intervertebral disk herniation	3 (7)	0 (0)
Bone marrow	44	17
Hemosiderosis	4 (9)	1 (6)
Hyperplasia, erythroid/megakaryocytic	1 (2)	0 (0)
Hyperplasia, myeloid/granulocytic*	3 (7)	6 (35)
Blood vessels (multiple tissues): polyarteritis**	15 (34)	0 (0)
Brain	44	18
Encephalitis, thromboembolic with bacteria	1 (2)	0 (0)
Gliosis, not otherwise specified	0 (0)	1 (6)
Inflammatory cell infiltrates/foci, perivascular	0 (0)	1 (6)
Melanosis, meninges	0 (0)	1 (6)
Mineralization, thalamus	4 (9)	2 (11)
Epididymis	39	18
Fibrosis	1 (3)	n/a
Inflammatory cell infiltrates/foci, interstitial	5 (13)	n/a
Pigment accumulation, lipofuscin	2 (5)	n/a
Sperm granuloma	1 (3)	n/a
Sperm stasis	8 (21)	n/a
Esophagus: megaesophagus	7 of 44 (16)	4 of 18 (22)
Eyes and eyelids	42	16
Blepharitis/blepharoconjunctivitis[b,c]	38 (91)	15 (94)
Keratitis[d]	2 (5)	0 (0)
Lens degeneration/cataract	0 (0)	1 (6)
Retinal detachment	1 (2)	1 (6)
Forestomach	44	18
Erosion/ulceration, mucosal	2 (5)	0 (0)
Hyperkeratosis/hyperplasia, mucosal	7 (16)	1 (6)
Inflammatory cell infiltrates/foci, lamina propria/submucosa	1 (2)	0 (0)
Gallbladder: hyperplasia with hyalinosis, epithelium	1 of 30 (3)	1 of 12 (8)
Glandular stomach	44	18
Erosion/ulceration, mucosal	4 (9)	3 (17)
Hyperplasia polypoid, mucosal	1 (2)	0 (0)
Hyperplasia with hyalinosis, mucosal	4 (9)	4 (22)
Hyperplasia with intestinal metaplasia, mucosal	6 (14)	5 (28)
Inflammatory cell infiltrates/foci, lamina propria/submucosa	3 (7)	0 (0)
Yeast	1 (2)	0 (0)
Harderian gland	42	16
Hyperplasia	5 (12)	3 (19)
Inflammatory cell infiltrates/foci, interstitial	7 (17)	3 (19)
Heart	44	18
Cardiomyopathy	25 (57)	8 (44)
Endocarditis, valvular with bacteria	2 (5)	0 (0)
Fibrosis, pericardial	0 (0)	1 (6)
Inflammatory cell infiltrates/foci, myocardial/epicardial	2 (5)	2 (11)
Melanosis, subendocardial	0 (0)	1 (6)
Mineralization, myocardial	3 (7)	0 (0)
Necrosis, myocardial	1 (2)	2 (11)
Pancarditis, suppurative with bacteria	2 (5)	2 (11)
Kidneys	43	18
Atrophy, tubular	3 (7)	0 (0)
Chronic nephropathy	3 (7)	0 (0)
Cysts, tubular	3 (7)	0 (0)
Degeneration/necrosis, tubular	6 (14)	0 (0)
Dilation/eosinophilic casts, tubular	13 (30)	3 (17)
Glomerulonephritis	3 (7)	0 (0)
Glomerulosclerosis	2 (5)	0 (0)

(continued)

Table 3. (continued)

Organ/Tissue and Lesion	Males	Females
Hyaline droplets, tubular	1 (2)	0 (0)
Hydronephrosis[e]	8 (19)	6 (33)
Hyperplasia with hyalinosis, pelvic transitional epithelium	0 (0)	2 (11)
Infarcts, cortical	3 (7)	0 (0)
Inflammatory cell infiltrates/foci, interstitial/perivascular	22 (51)	13 (72)
Nephritis, suppurative with bacteria/bacterial emboli	5 (12)	2 (11)
Pyelitis	0 (0)	2 (11)
Large intestine	44	18
Inflammatory cell infiltrates/foci, lamina propria/submucosa	1 (2)	0 (0)
Pinworm nematodes	5 (11)	5 (28)
Liver	44	18
Angiectasis	3 (7)	2 (11)
Degeneration, hepatocellular	11 (25)	2 (11)
Extramedullary hematopoiesis***	4 (9)	12 (67)
Fibrosis	0 (0)	1 (6)
Focus of cellular alteration, hepatocellular	1 (2)	0 (0)
Hyperplasia with hyalinosis, bile duct	3 (7)	3 (17)
Hyperplasia, sinusoidal lining cells	1 (2)	0 (0)
Inflammatory cell infiltrates/foci, portal/intralobular/centrilobular	19 (43)	7 (39)
Karyocytomegaly, hepatocellular	6 (14)	0 (0)
Lobe torsion with infarction	1 (2)	0 (0)
Necrosis, hepatocellular	2 (5)	3 (17)
Regenerative hyperplasia, hepatocellular	3 (7)	2 (11)
Thrombosis/hemorrhage	2 (5)	0 (0)
Lungs	44	18
Eosinophilic crystalline pneumonia	26 (59)	11 (61)
Eosinophilic crystals, bronchial/alveolar	30 (68)	13 (72)
Hemorrhage	1 (2)	0 (0)
Inflammation, suppurative	1 (2)	1 (6)
Inflammatory cell infiltrates/foci, perivascular/peribronchial	5 (11)	3 (17)
Thrombosis/necrosis	0 (0)	1 (6)
Lymph nodes	32	13
Depletion, lymphoid	8 (25)	3 (23)
Extramedullary hematopoiesis, increased	0 (0)	2 (15)
Hemosiderosis	8 (25)	0 (0)
Hyperplasia, lymphoid	9 (28)	3 (23)
Lymphadenitis	3 (9)	2 (15)
Plasmacytosis*	6 (19)	8 (62)
Sinus dilation	3 (9)	0 (0)
Sinus histiocytosis	12 (38)	4 (31)
Mammary gland		15
Galactocele	n/a	3 (20)
Inflammatory cell infiltrates/foci, perivascular/periductal	n/a	1 (7)
Ovary		8
Atrophy	n/a	4 (50)
Cyst	n/a	5 (63)
Hematocyst	n/a	3 (38)
Hyperplasia, tubulostromal	n/a	1 (13)
Inflammatory cell infiltrates/foci, stroma/mesovarium	n/a	5 (63)
Pancreas	44	18
Atrophy, exocrine compartment	1 (2)	0 (0)
Cyst, ductal	0 (0)	2 (11)
Fibrosis	0 (0)	1 (6)
Hyperplasia with hyalinosis, ductal	1 (2)	0 (0)
Inflammatory cell infiltrates/foci, interstitial	2 (5)	1 (6)
Preputial gland: adenitis, suppurative[f]	10 (23)	n/a
Prostate	7	
Dilation, acinar	3 (43)	n/a
Inflammation, suppurative	1 (14)	n/a

(continued)

Table 3. (continued)

Organ/Tissue and Lesion	Males	Females
Skeletal muscle	43	18
Degeneration, myofiber	1 (2)	0 (0)
Fibrosis	1 (2)	0 (0)
Inflammation, suppurative (abscess)	2 (5)	0 (0)
Small intestine	44	18
Amyloidosis	1 (2)	0 (0)
Enteritis, suppurative and/or ulcerative	2 (5)	0 (0)
Inflammatory cell infiltrates/foci, lamina propria/submucosa	3 (7)	1 (6)
Spinal cord: spinal cord, hemorrhage	0 (0)	1 (6)
Spleen	43	18
Depletion, lymphoid	9 (21)	8 (44)
Extramedullary hematopoiesis, increased***	2 (5)	8 (44)
Hemosiderosis	5 (12)	3 (17)
Hyperplasia, lymphoid	0 (0)	1 (6)
Plasmacytosis	2 (5)	3 (17)
Seminal vesicles	14	
Dilation	11 (79)	n/a
Inflammation, suppurative[g]	7 (50)	n/a
Torsion/hemorrhage	1 (7)	n/a
Skin	35	15
Abscess, subcutis/fascia	1 (3)	0 (0)
Atrophy, adnexal	1 (3)	3 (20)
Dermatitis chronic with acanthosis and hyperkeratosis[h]	9 (26)	6 (40)
Dermatophytosis	1 (3)	0 (0)
Hematoma, subcutis	1 (3)	0 (0)
Inflammatory cell infiltrates/foci, dermis	4 (11)	3 (20)
Mites	8 (23)	5 (33)
Panniculitis	1 (3)	0 (0)
Squamous epithelial cyst	1 (3)	0 (0)
Ulceration	0 (0)	1 (7)
Testes	39	
Atrophy, seminiferous tubules	4 (10)	n/a
Necrosis, seminiferous tubules	1 (3)	n/a
Pigment accumulation, lipofuscin	1 (3)	n/a
Urinary bladder	8	4
Cystitis, lymphofollicular*	0 (0)	3 (75)
Cystitis, necrosuppurative with bacteria	0 (0)	1 (25)
Proteinaceous plug	2 (25)	0 (0)
Uterus		17
Adenomyosis	n/a	2 (12)
Angiectasis/thrombosis	n/a	9 (53)
Hyperplasia endometrial cystic	n/a	12 (71)
Metritis/pyometra[i]	n/a	8 (47)

Abbreviation: n/a, not applicable.
[a]Data are reported as number of affected mice per total number of examined mice (%).
[b]In 19 males and 11 females, Gram-positive rods were observed in association with this lesion.
[c]Lesion occurred bilaterally in 31 males and 15 females.
[d]Lesion occurred bilaterally in 1 male.
[e]Lesion occurred bilaterally in 1 male and 1 female.
[f]Intralesional bacteria were observed in 5 cases; the lesion was complicated by cellulitis in 4 cases.
[g]Intralesional bacteria were observed in 4 cases; the lesion was complicated by peritonitis in 1 case.
[h]Pustular lesions with intralesional bacteria were observed in 3 cases.
[i]Intralesional bacteria were observed in 4 cases; the lesion was complicated by peritonitis in 4 cases.
*$P < .05$. **$P < .01$. ***$P < .001$. Difference between males and females.

frequent uterine lesions being observed in about half of the females (Fig. 12). In addition, peritonitis was identified as a lethal complication of suppurative metritis/pyometra in 4 females.

Fibro-osseous lesion (FOL) was another relatively frequent nonneoplastic change that was almost exclusively observed in females (8 of 17 females but only 1 of 44 males). Early lesions were identified in few cases, mainly affecting epiphyseal/

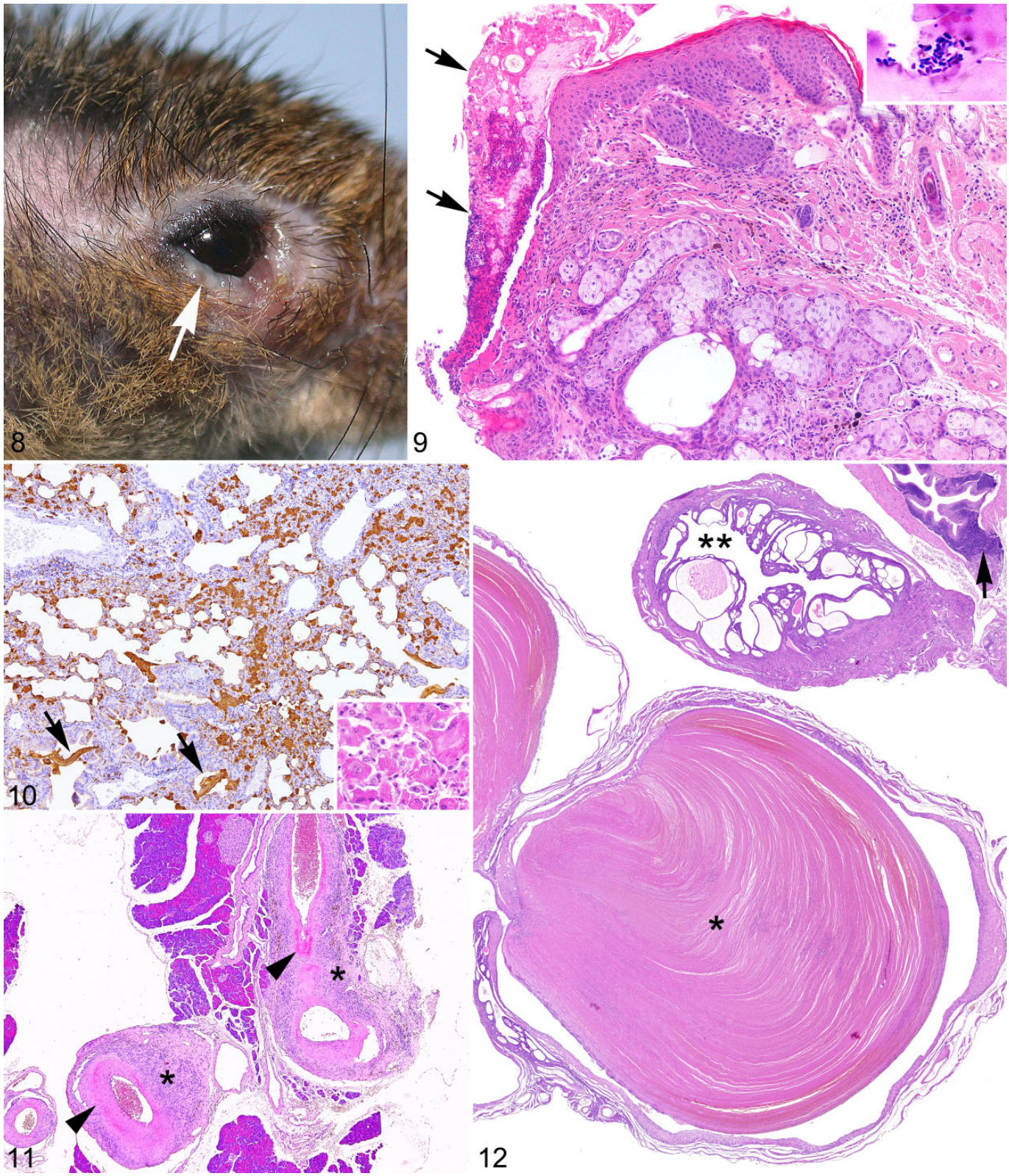

Figures 8–12. Major nonneoplastic lesions affecting 129S6/SvEvTac mice. **Figure 8.** Suppurative and ulcerative blepharoconjunctivitis, male mouse. The eye has suppurative discharge with ulceration of the lower eyelid (arrow). **Figure 9.** Suppurative and ulcerative blepharoconjunctivitis, male mouse. The mucocutaneous junction of the eyelid is ulcerated with chronic suppurative inflammation and extensive serocellular crusting (arrows). Hematoxylin and eosin (HE). Inset: Clusters of curved rod-shaped bacteria populate the serocellular crusts. Gram stain. **Figure 10.** Eosinophilic crystalline pneumonia, male mouse. The lesion consists of parenchymal infiltrates of Chi3l3/Ym1-positive macrophages,

metaphyseal extremities of long bones and characterized by irregular proliferations of dense fibrovascular tissue with extensive effacement of bone marrow and osteoclastic trabecular bone resorption. In most instances, advanced lesions with clear osteosclerotic progression were noted, showing bone marrow spaces almost completely obscured by thick bony trabeculae (Suppl. Fig. 10).

Other minor changes reported with a significantly higher frequency in females included foci of extramedullary hematopoiesis in the liver, increased extramedullary hematopoiesis in the splenic red pulp, lymphoid depletion affecting the splenic white pulp, reactive myeloid hyperplasia of the bone marrow, and plasmacytosis in the lymph nodes.

Minimal to mild infiltrates or foci of inflammatory cells were detected in a wide range of tissues, with the most frequent nonneoplastic changes being observed in the liver of males (19 of 44, 43%) and the kidneys of both sexes (22 of 43 for males, 51%; 13 of 18 for females, 72%).

Ovaries and lower urogenital tract, including urinary bladder and most of male accessory sex glands, were not consistently analyzed histologically or were sometimes included in the evaluation only when affected by grossly detectable changes. Thus, the prevalence of lesions in these organs cannot be inferred with accuracy.

Causes of Death/Contributory Causes of Death

Major CCODs are summarized in Table 4. Hematopoietic tumors were the most common neoplastic conditions noted as single major COD in males, followed by hepatocellular and gastrointestinal tumors. One male succumbed to an anaplastic metastatic tumor apparently arising from a testicle. Immunohistochemistry failed to support a definitive classification of this neoplasm. Tumors identified as single major COD in females included an adenocarcinoma of the Harderian gland characterized by invasion of the skull and brain and metastatic dissemination to the lungs, a hemangiosarcoma arising in the skin of the tail with pulmonary and hepatic metastases, an adenoma of the pituitary pars distalis, and a lymphoma with multisystemic dissemination.

Nonneoplastic CCODs included polyarteritis, ECP, urologic syndrome, peritonitis resulting from suppurative and necrotizing seminal vesiculitis, suppurative metritis/pyometra (in most cases with associated peritonitis), sepsis (Suppl. Fig. 11), and megaesophagus. In several instances, multiple disease conditions were identified as concurrent CCODs (Table 4). In this context, polyarteritis, cardiomyopathy, and preputial gland suppurative adenitis/abscessation were noted as relevant comorbidities in males (Suppl. Fig. 12). Megaesophagus was noted as significant comorbidity in 4 males and 1 female. ECP was identified as comorbidity along with pulmonary adenocarcinoma and other nonneoplastic conditions in 4 males. ECP was also noted as a CCOD in 2 females, in both cases in association with uterine angiectasis/thrombosis. Presence of a uterine tumor (hemangioma) and development of sepsis were also considered significant comorbidities in these 2 mice. Ependymomas noted in the brain of 3 males were considered a CCOD but in all cases as comorbidities associated with concurrent nonneoplastic lesions.

Table 4. Major CCOD in Aging Male and Female 129S6/SvEvTac Mice, *n* (%).[a]

CCOD	Males ($n = 44$)	Females ($n = 18$)
Neoplastic CCOD		
Hematopoietic	5 (11)	1 (6)
Harderian gland	0 (0)	1 (6)
Gastrointestinal	2 (5)	0 (0)
Liver	2 (5)	0 (0)
Vascular	0 (0)	1 (6)
Pituitary	0 (0)	1 (6)
Other malignant metastatic tumor	1 (2)	0 (0)
Total	10 (23)	4 (22)
Nonneoplastic CCOD		
Polyarteritis	5 (11)	0 (0)
Eosinophilic crystalline pneumonia	4 (9)	2 (11)
Megaesophagus	1 (2)	0 (0)
Sepsis	2 (5)	2 (11)
Suppurative metritis/pyometra/peritonitis	n/a	4 (22)
Uterine angiectasis/thrombosis	n/a	1 (6)
Urologic syndrome	2 (5)	0 (0)
Necrosuppurative cystitis and hydronephrosis	0 (0)	1 (6)
Seminal vesicle suppurative adenitis	1 (2)	n/a
Total	15 (34)	10 (56)
Multiple causes or comorbidities		
Multiple concurrent nonneoplastic causes	10 (23)	1 (6)
Concurrent neoplastic and nonneoplastic causes	7 (16)	3 (17)
Total	17 (39)	4 (22)
Undetermined CCOD	2 (5)	0 (0)

Abbreviations: CCOD, contributory cause of death; n/a, not applicable.
[a]Results are presented as number of affected mice per total number of examined mice (%).

Discussion

We report a longitudinal aging study of 129S6/SvEvTac mice describing the spectrum of spontaneous age-related disorders

Figure 10. (continued) and elongated extracellular Chi3l3/Ym1-positive crystals are scattered in the lumen of bronchioles and alveoli (arrows). Immunohistochemistry for Chi3l3/Ym1 protein. Inset: The macrophages have intracytoplasmic accumulation of eosinophilic crystalline material. HE. **Figure 11.** Polyarteritis, pancreas, male mouse. Medium-sized arteries have prominent hypertrophy and fibrinoid necrosis of the tunica media (arrowheads) associated with fibrosis and inflammatory cell infiltrates expanding the adventitial layer (asterisks). HE. **Figure 12.** Urogenital tract lesions, female mouse. There is angiectasis and thrombosis of a myometrial/endometrial vein (asterisk). Changes consistent with cystic endometrial hyperplasia are present in an adjacent segment of the uterus (double asterisk). The urinary bladder has dense lymphofollicular infiltrates expanding the submucosa (arrow). HE.

occurring in 44 males and 18 females. While our study was mainly focused on defining the nature and frequency of age-related lesions at the pathologic level, other relevant end points have been investigated, including major contributory causes of morbidity and death, clinical manifestations, and longevity (life span).

Epithelial tumors of the Harderian gland and lung were the most common neoplastic lesions encountered in both sexes, as previously described in aging 129S4/SvJae mice.[72] Murine Harderian gland and bronchioloalveolar compartment are preferential targets of oncogenic *K-ras* and *H-ras* activity. The correlation between activating *K-ras* mutations and concurrent development of epithelial tumors from both locations has been widely documented in carcinogenicity studies.[23,57,58] A role for *H-ras* oncogene during pulmonary and/or Harderian gland tumorigenesis has been demonstrated in spontaneously occurring cases as well as in transgenic mice overexpressing the human *c-Ha-ras* oncogene.[5,18,39] Interestingly, proclivity for the development of spontaneous pulmonary tumors in the 129X1/SvJ mouse appears to be directly linked with a specific pulmonary adenoma susceptibility 1 (*Pas1*) haplotype that leads to constitutive overexpression of *K-ras* in the lung.[7,68] Thus, a similar molecular mechanism might be responsible for the high incidence of lung and Harderian gland tumors observed in other 129 substrains.

Similar to what is reported for the 129S4/SvJae substrain, hematopoietic tumors rarely occurred in 129S6/SvEvTac mice.[72] Despite their low frequency, hematopoietic malignancies represented an important COD because of their disseminated nature with extensive involvement of multiple organ and tissues. Notably, we identified an unusual but distinctive case of disseminated mast cell sarcoma. A large multinodular mass in the dermis/subcutis was tentatively identified as the primary lesion. However, because of the extensive involvement of most of the examined organs/tissues, the actual site of tumor origin could not be ascertained, and a possible multicentric origin of the lesion was considered. The mast cell disorder reported in the 129S6/SvEvTac mouse recapitulates some of the most representative pathobiologic features of systemic mastocytosis in humans, including concurrent cutaneous involvement and dissemination to visceral organs and bone marrow.[34] Although a series of proliferative mast cell disorders have been documented in chemically induced or genetically engineered mouse models,[17,34,41,65] naturally occurring lesions remain exceedingly rare.[15] Description of spontaneous mast cell tumors is limited to sporadic cases in diverse mouse strains, including CD-1, BALB/c, B6C3F1, CFLP, C57BL/6, and 4-way cross mice.[6,14,15,28,30] Similarly to what has been observed in our study, the majority of these spontaneous lesions exhibited an aggressive behavior with systemic dissemination at the level of skin, bone marrow, and visceral organs.

Ependymoma, another unique neoplasm here diagnosed in 3 males, is considered an exceedingly rare spontaneous lesion in the mouse.[1,25] A recent retrospective database analysis identified 3 cases of ependymoma on >100 000 mice surveyed.[1] In view of these data, the prevalence of ependymomas observed in our cohort is unexpectedly high. Analysis of a larger number of aging animals may clarify whether a real predisposition for ependymal neoplasms exists in the 129S6/SvEvTac substrain. Microscopically, all 3 showed typical diagnostic features of a rodent ependymoma, including periventricular distribution, prominent vascular network (microvascular proliferation), and perivascular pseudorosettes without evidence of luminal rosettes. All 3 ependymomas were designed as malignant based on intratumoral necrosis and/or invasion of the surrounding neuroparenchyma.[1,25] Immunohistochemical examination confirmed lack of glial fibrillary acidic protein expression and diffuse vimentin positivity, features characteristic for rodent ependymoma.[1] In addition, individual tumor cells displayed unequivocal cytoplasmic wide-spectrum cytokeratin immunoreactivity, as seen in ependymal tumors of humans, cats, and dogs.[35,55,69,74]

In our study, an accurate comparison of tumor frequencies between sexes is limited by the smaller female cohort. Nevertheless, major sex-related variations could be identified for some of the most frequent neoplastic categories. Despite an overall higher prevalence of Harderian gland tumors in males, malignant lesions were more commonly reported in females where they showed a particularly aggressive behavior, with local invasion of the skull and brain and metastatic spread to the lungs observed in one case. The same higher male prevalence of Harderian gland tumors was described also in 129S4/SvJae mice, but malignant lesions occurred only sporadically in this substrain without clear differences between sexes.[3,72]

Primary pulmonary tumors were more frequent in 129S6/SvEvTac females than males. This apparent female predisposition is in contrast with other data reported for aging 129S4/SvJae mice.[3,72]

For hepatocellular tumors, 129S6/SvEvTac males were more frequently affected than females. Furthermore, malignant lesions (hepatocellular carcinomas) occurred only in males where they represented an important COD/CCOD. Increased male susceptibility to spontaneous hepatocellular tumors is obvious in most inbred mouse strains, including the 129S4/SvJae substrain, as in other species, including humans.[3,48,72] Male predisposition is seen not only in the context of spontaneous hepatic tumorigenesis but also in diverse experimental settings, including the induction of liver tumors by a wide variety of carcinogens or infectious agents.[4,47] Endocrine ablation studies have demonstrated that sexual differences in susceptibility results from the opposing effects of male and female sex hormones, with testosterone enhancing and ovarian hormones and prolactin inhibiting hepatocellular tumor development.[4,21]

Blepharitis/blepharoconjunctivitis represented by far the most prevalent nonneoplastic age-related disorder affecting both male and female 129S6/SvEvTac mice, but it has been only occasionally reported in laboratory mice.[60] Ulcerative blepharoconjunctivitis is an age-related disorder that appears to be more common in BALB/c, C57BL/6, and 129P3/J than other inbred lines of mice.[43] A variety of opportunistic bacteria (eg, *Corynebacterium* spp, *Staphylococcus aureus*, *Staphylococcus xylosus*, *Pasteurella pneumotropica*) have been

identified during episodes of blepharoconjunctivitis, although their role in pathogenesis is still matter of controversy.[63] Corynebacteria in particular have been identified in outbreaks involving aging mice.[43,60,63] In one study of spontaneous blepharoconjunctivitis in a colony of 129P3/J mice, the prevalence in both sexes increased progressively to approximately 50% at ≥30 weeks of age.[63] An uncharacterized corynebacterial species was consistently isolated from the affected eyes.[63] An epizootic of ulcerative conjunctivitis and keratitis associated with an unidentifiable *Corynebacterium* spp was also reported in a colony of male C57BL/6 mice. Ocular lesions were first detected at 18 months of age, and their incidence and severity increased dramatically to involve >90% of 21- to 30-month-old mice.[33]

In our study, diverse corynebacterial species were commonly isolated from ocular lesions. However, data from follow-up clinicopathologic and microbiological investigations do not support an unequivocal causal association between bacteria and blepharitis/blepharoconjunctivitis. All the identified corynebacterial species have been described as common inhabitants of mouse skin without a specific pathogenic role in immunocompetent hirsute mice.[10,11,16,40,49,51] The reason for their frequent recovery from the conjunctiva and their role in the development and progression of ocular lesions are currently undetermined. We hypothesize that age-related structural and/or functional changes in the eyelids and lacrimal system may have impaired the integrity of the mucocutaneous epithelial barrier, thus promoting chronic inflammation and facilitating the colonization of the palpebral conjunctiva by commensal bacteria normally residing on the skin.[33,43,45] Further supporting this view, anterior migration of the palpebral mucocutaneous junction represents a well-documented age-related condition in mice where it is mainly associated with eyelid laxity and meibomian gland atrophy and dysfunction.[42,61] Furthermore, our data suggest that concurrent Harderian gland tumors contribute significantly to the exacerbation, rather than to the onset, of blepharoconjunctivitis.

ECP, formerly known as acidophilic macrophage pneumonia, has been described as a major cause of disease and death in C57BL/6 mutant mice deficient in SHP-1 protein-tyrosine phosphatase (''motheaten'' and ''viable motheaten'').[56,71] ECP has been reported with variable incidence in different mouse strains[38]; it has also been characterized as a frequent pulmonary lesion and significant cause of morbidity and mortality in 129S4/SvJae mice.[22,72,73] Cytoplasmic hyaline change, commonly referred to as ''hyalinosis,'' affecting the epithelium of the nasal respiratory and olfactory mucosa, the trachea and bronchi (with or without concurrent ECP), glandular stomach, bile duct, and pancreatic duct, has been reported in mice of the 129S4/SvJae substrain and in the B6;129 mouse line.[72,73] The intrahistiocytic and extracellular eosinophilic crystals in ECP and epithelial hyalinosis consist of mammalian chitinase-like lectin proteins of the Ym family.[19,73]

In our study, pulmonary accumulation of eosinophilic crystals and ECP were frequent in males and females, often occurring together. ECP was a major COD/CCOD in both sexes. Epithelial hyalinosis in extrapulmonary sites was more prevalent in 129S6/SvEvTac females, similar to that reported in the 129S4/SvJae subline.[72,73] In our study, hyaline change was recorded in the epithelium of glandular stomach, bile ducts, gall bladder, and pancreatic duct. Hyalinosis and hyperplasia of the transitional epithelium of the renal pelvis were noted in 2 females in association with inflammation or hydronephrosis. Other studies have described a similar lesion. Upregulated expression and accumulation of Chi3l3/Ym1 proteins have been reported in a polypoid adenoma of the transitional epithelium of the renal pelvis in a *PML/RAR*α knock-in mouse with acute myeloid leukemia[31] and in the hyperplastic transitional epithelium in F2 progeny of C57BL/6 and DBA/2 mice with ureteritis and hydronephrosis.[24] Immunohistochemistry confirmed accumulation of Chi3l3/Ym1 within macrophages and in extracellular crystals within bronchial/alveolar lumens in ECP and in epithelial cells affected by hyalinosis in the above-mentioned tissues.

Major nonneoplastic conditions with an obvious sex predisposition included FOL and polyarteritis. While FOL represented a frequent disorder in 129S6/SvEvTac females (8 of 17 affected females), only 1 case was confirmed in males, as previously described.[2,50,70] The pathogenesis of this condition appears to be driven by age-related imbalances of female reproductive hormones. Some mouse lines (including the 129S4/SvJae substrain) are reportedly more susceptible than others, indicating that specific genetic backgrounds may further enhance the hormonal impact.[2,70,72] Experimental evidence supporting these mechanisms were provided by the observation that synthetic compounds with hormonal activity like diethylstilbestrol and misoprostol also induce a high incidence of FOL in female mice, while males are only marginally affected.[32] A causal association has been proposed between other age-related lesions of female reproductive tract (eg, ovarian atrophy, ovarian cysts, cystic endometrial hyperplasia) and development FOL.[2,9,70] A similar correlation could not be confirmed in our study, since all the examined females were ultimately affected by multiple and often concurrent uterine and ovarian lesions.

A distinctive proclivity for the development of polyarteritis was observed in 129S6/SvEvTac males, but the same condition was never reported in females. For their severity (especially when affecting vital organs) and multisystemic nature, vascular lesions were often considered a significant CCOD. An obvious male predisposition for arteritis has also been documented in the 129S4/SvJae substrain, while an opposite trend was noted in B6;129 mice.[3,20,72] Immune-mediated mechanisms have been proposed in the pathogenesis of spontaneous polyarteritis in aging mice.[43,45] In this context, lifelong expression of proteins encoded by endogenous retroviruses/retroelements has been considered as the event potentially responsible for most of the immune-mediated disorders in aging mice, including glomerulonephritis and polyarteritis.[36,43,64] However, hypertension may also have a primary role in the development of murine polyarteritis.[37] Interestingly, in a study of 11 commonly used inbred mouse strains, male 129S1/SvImJ mice

exhibited the highest systolic blood pressure.[8] Given the assumption that the same male-predominant high blood pressure phenotype is equally represented among different 129 substrains, hypertension in aging 129S6/SvEvTac males might be involved in the pathogenesis of polyarteritis.

As frequently observed in other mouse strains, including 129S4/SvJae and B6;129 mice,[20,72] chronic progressive cardiomyopathy emerged as an age-related disorder in 129S6/SvEvTac mice with overall comparable incidence in male and females. Different degrees of myocardial involvement were recognized, with more severe lesions considered a CCOD in males.

In both sex groups of 129S6/SvEvTac mice, suppurative inflammation of the urogenital tract and accessory sex glands (with or without evidence of bacterial infection) was a frequent lesion and an important COD/CCOD. The condition in females was mainly characterized by pyometra or suppurative metritis, often evolving to peritonitis as a lethal complication. Abscessation of the preputial gland was the most common manifestation in males, whereas necrosuppurative inflammation of the seminal vesicles or prostate occurred at lower frequency. Cellulitis/fasciitis of the inguinopubic region and peritonitis represented clinically relevant and perhaps lethal complications of lesions affecting preputial glands and seminal vesicles, respectively. A variety of opportunistic bacteria, including *Pasteurella pneumotropica*, *Klebsiella oxytoca*, and staphylococci, are normally responsible for the development suppurative lesions affecting the urogenital tract and accessory sex glands.[43,46] Unfortunately, the cases reported in our study were not investigated microbiologically.

In conclusion, this study identifies the major neoplastic and nonneoplastic conditions affecting aging 129S6/SvEvTac mice; their distribution and frequency are similar to those previously reported for other 129 substrains.[3,63,72] In addition, our data confirm that the 129 background is actually ''resistant'' to a series of classical age-related disorders (including hematopoietic and mammary tumors, amyloidosis, rectal prolapse, and dermatitis) commonly encountered in other strains of mice, including backcrossed 129 lines.[3,20,43,45,72] Overall, these findings reinforce the idea that, while a high degree of genetic variability exists within the 129 strain, major age-related phenotypic traits are equally represented over several substrains. This work defines the spontaneous or ''background'' pathology of a 129 substrain that has been widely used for the generation of targeted mutant mouse lines and should therefore be of value for the interpretation of spontaneous aging lesions in inbred 129S6/SvEvTac mice and incompletely backcrossed strains where targeted mutation has been originally generated in 129S6/SvEvTac mice embryonic stem cells.

Acknowledgements

We are grateful for the excellent technical assistance of Maurizio Barzani, Marco Brevi (Department of Veterinary Sciences and Public Health, University of Milan, Milan, Italy), Marco Losa (Mouse and Animal Pathology Laboratory, Filarete Foundation, Milan, Italy), and Annick Francis (InfraMouse, KU Leuven-VIB, Leuven, Belgium).

Declaration of Conflicting Interests

The authors declared no potential conflicts of interest with respect to the research, authorship, and/or publication of this article.

Funding

The author(s) received no financial support for the research, authorship, and/or publication of this article.

References

1. Adams ET, Auerbach S, Blackshear PE, et al. Proceedings of the 2010 National Toxicology Program Satellite Symposium. *Toxicol Pathol*. 2011; **39**:240–266.
2. Albassam MA, Wojcinski ZW, Barsoum NJ, et al. Spontaneous fibro-osseous proliferative lesions in the sternums and femurs of B6C3F1 mice. *Vet Pathol*. 1991;**28**:381–388.
3. Brayton CF, Treuting PM, Ward JM. Pathobiology of aging mice and GEM: background strains and experimental design. *Vet Pathol*. 2012;**49**: 85–105.
4. Bugni JM, Poole TM, Drinkwater NR. The little mutation suppresses DEN-induced hepatocarcinogenesis in mice and abrogates genetic and hormonal modulation of susceptibility. *Carcinogenesis*. 2001;**22**:1853–1862.
5. Candrian U, You M, Goodrow T, et al. Activation of protooncogenes in spontaneously occurring non-liver tumors from C57BL/6 x C3 H F1 mice. *Cancer Res*. 1991;**51**:1148–1153.
6. Chrisp CE, Turke P, Luciano A, et al. Lifespan and lesions in genetically heterogeneous (four-way cross) mice: a new model for aging research. *Vet Pathol*. 1996;**33**:735–743.
7. Dassano A, Colombo F, Trincucci G, et al. Mouse pulmonary adenoma susceptibility 1 locus is an expression QTL modulating Kras-4A. *PLoS Genet*. 2014;**10**: e1004307.
8. Deschepper CF, Olson JL, Otis M, et al. Characterization of blood pressure and morphological traits in cardiovascular-related organs in 13 different inbred mouse strains. *J Appl Physiol (1985)*. 2004;**97**:369–376.
9. Dodd DC, Port CD. Hyperostosis of the marrow cavity caused by misoprostol in CD-1 strain mice. *Vet Pathol*. 1987;**24**:545–548.
10. Dole VS, Henderson KS, Fister RD, et al. Pathogenicity and genetic variation of 3 strains of *Corynebacterium bovis* in immunodeficient mice. *J Am Assoc Lab Anim Sci*. 2013;**52**:458–466.
11. Duga S, Gobbi A, Asselta R, et al. E: Analysis of the 16 S rRNA gene sequence of the coryneform bacterium associated with hyperkeratotic dermatitis of athymic nude mice and development of a PCR-based detection assay. *Mol Cell Probes*. 1998;**12**:191–199.
12. Elwell MR, Mahler JF. Heart, blood and lymphatic vesselsIn: Maronpot RR, Boorman GA, Gaul BW, eds. *Pathology of the Mouse: Reference and Atlas*. Vienna, IL: Cache River Press; 1999:361–380.
13. Festing MF, Simpson EM, Davisson MT, et al. Revised nomenclature for strain 129 mice. *Mamm Genome*. 1999;**10**:836.
14. Frith CH, Sprowls RW, Breeden CR. Mast cell neoplasia in mice. *Lab Anim Sci*. 1976;**26**:478–481.
15. Frith CH, Ward JM, Chandra M. The morphology, immunohistochemistry, and incidence of hematopoietic neoplasms in mice and rats. *Toxicol Pathol*. 1993; **21**:206–218.
16. Gobbi A, Crippa L, Scanziani E. *Corynebacterium bovis* infection in immunocompetent hirsute mice. *Lab Anim Sci*. 1999;**49**:209–211.
17. Godfraind C, Louahed J, Faulkner H, et al. Intraepithelial infiltration by mast cells with both connective tissue-type and mucosal-type characteristics in gut, trachea, and kidneys of IL-9 transgenic mice. *J Immunol*. 1998;**160**: 3989–3996.
18. Goodrow TL, Nichols WW, Storer RD, et al. Activation of H-ras is prevalent in 1,3-butadiene-induced and spontaneously occurring murine Harderian gland tumors. *Carcinogenesis*. 1994;**15**:2665–2667.

19. Guo L, Johnson RS, Schuh JC. Biochemical characterization of endogenously formed eosinophilic crystals in the lungs of mice. *J Biol Chem*. 2000;**275**: 8032–8037.
20. Haines DC, Chattopadhyay S, Ward JM. Pathology of aging B6;129 mice. *Toxicol Pathol*. 2001;**29**:653–661.
21. Hartwell HJ, Petrosky KY, Fox JG, et al. Prolactin prevents hepatocellular carcinoma by restricting innate immune activation of c-Myc in mice. *Proc Natl Acad Sci U S A*. 2014;**111**:11455–11460.
22. Hoenerhoff MJ, Starost MF, Ward JM. Eosinophilic crystalline pneumonia as a major cause of death in 129S4/SvJae mice. *Vet Pathol*. 2006;**43**: 682–688.
23. Hong HH, Houle CD, Ton TV, et al. K-ras mutations in lung tumors and tumors from other organs are consistent with a common mechanism of ethylene oxide tumorigenesis in the B6C3F1 mouse. *Toxicol Pathol*. 2007;**35**:81–85.
24. Ichii O, Otsuka S, Namiki Y, et al. Molecular pathology of murine ureteritis causing obstructive uropathy with hydronephrosis. *PLoS One*. 2011;**6**: e27783.
25. Kaufmann W, Bolon B, Bradley A, et al. Proliferative and nonproliferative lesions of the rat and mouse central and peripheral nervous systems. *Toxicol Pathol*. 2012;**40**:87S–157S.
26. Kodell RL, Blackwell BN, Bucci TJ, et al. Cause-of-death assignment at the National Center for Toxicological Research. *Toxicol Pathol*. 1995;**23**: 241–247.
27. Latendresse JR, Warbrittion AR, Jonassen H, et al. Fixation of testes and eyes using a modified Davidson's fluid: comparison with Bouin's fluid and conventional Davidson's fluid. *Toxicol Pathol*. 2002;**30**:524–533.
28. Lewis DJ, Offer JM. Malignant mastocytoma in mice. *J Comp Pathol*. 1984;**94**: 615–620.
29. Livrozet M, Vandermeersch S, Mesnard L, et al. An animal model of type A cystinuria due to spontaneous mutation in 129S2/SvPasCrl mice. *PLoS One*. 2014;**9**:e102700.
30. Majeed SK. Mast cell tumours in CD-1 mice. *Arzneimittelforschung*. 1991;**41**: 175–178.
31. Marchesi F, Minucci S, Pelicci PG, et al. Immunohistochemical detection of Ym1/Ym2 chitinase-like lectins associated with hyalinosis and polypoid adenomas of the transitional epithelium in a mouse with acute myeloid leukemia. *Vet Pathol*. 2006;**43**:773–776.
32. McAnulty PA, Skydsgaard M. Diethylstilbestrol (DES): carcinogenic potential in Xpa-/-, Xpa-/- / p53+/-, and wild-type mice during 9 months' dietary exposure. *Toxicol Pathol*. 2005;**33**:609–620.
33. McWilliams TS, Waggie KS, Luzarraga MB, et al. *Corynebacterium* species–associated keratoconjunctivitis in aged male C57BL/6 J mice. *Lab Anim Sci*. 1993;**43**:509–512.
34. Merz H, Kaehler C, Hoefig KP, et al. Interleukin-9 (IL-9) and NPM-ALK each generate mast cell hyperplasia as single "hit" and cooperate in producing a mastocytosis-like disease in mice. *Oncotarget*. 2010;**1**:104–119.
35. Michimae Y, Morita T, Sunagawa Y, et al. Anaplastic ependymoma in the cervical spinal cord of a maltese dog. *J Vet Med Sci*. 2004;**66**:1155–1158.
36. Miyazawa M, Tabata N, Fujisawa R, et al. Roles of endogenous retroviruses and platelets in the development of vascular injury in spontaneous mouse models of autoimmune diseases. *Int J Cardiol*. 2000;**75**(suppl 1):S65–S73.
37. Mullink JW, Haneveld GT. Polyarteritis in mice due to spontaneous hypertension. *J Comp Pathol*. 1979;**89**:99–106.
38. Murray AB, Luz A. Acidophilic macrophage pneumonia in laboratory mice. *Vet Pathol*. 1990;**27**:274–281.
39. Nambiar PR, Turnquist SE, Morton D. Spontaneous tumor incidence in rasH2 mice: review of internal data and published literature. *Toxicol Pathol*. 2012; **40**:614–623.
40. Nieto E, Vindel A, Valero-Guillen PL, et al. Biochemical, antimicrobial susceptibility and genotyping studies on *Corynebacterium urealyticum* isolates from diverse sources. *J Med Microbiol*. 2000;**49**:759–763.
41. Ohmori T, Mori H, Rivenson A. A study of tobacco carcinogenesis XX: mastocytoma induction in mice by cigarette smoke particulates ("cigarette tar"). *Am J Pathol*. 1981;**102**:381–387.
42. Parfitt GJ, Xie Y, Geyfman M, et al. Absence of ductal hyper-keratinization in mouse age-related meibomian gland dysfunction (ARMGD). *Aging (Albany NY)*. 2013;**5**:825–834.
43. Percy DH, Barthold SW. Mouse. In: Percy DH, Barthold SW, eds. *Pathology of Laboratory Rodents and Rabbits*. 3rd ed. Ames, IA: Blackwell Publishing; 2007:3–124.
44. Peters LL, Robledo RF, Bult CJ, et al. The mouse as a model for human biology: a resource guide for complex trait analysis. *Nat Rev Genet*. 2007; **8**:58–69.
45. Pettan-Brewer C, Treuting PM. Practical pathology of aging mice. *Pathobiol Aging Age Relat Dis*. 2011;**1**.
46. Radaelli E, Manarolla G, Pisoni G, et al. Suppurative adenitis of preputial glands associated with *Corynebacterium mastitidis* infection in mice. *J Am Assoc Lab Anim Sci*. 2010;**49**:69–74.
47. Rogers AB, Boutin SR, Whary MT, et al. Progression of chronic hepatitis and preneoplasia in *Helicobacter hepaticus*–infected A/JCr mice. *Toxicol Pathol*. 2004;**32**:668–677.
48. Rogers AB, Theve EJ, Feng Y, et al. Hepatocellular carcinoma associated with liver-gender disruption in male mice. *Cancer Res*. 2007;**67**:11536–11546.
49. Russo M, Invernizzi A, Gobbi A, et al. Diffuse scaling dermatitis in an athymic nude mouse. *Vet Pathol*. 2013;**50**:722–726.
50. Sass B, Montali RJ. Spontaneous fibro-osseous lesions in aging female mice. *Lab Anim Sci*. 1980;**30**:907–909.
51. Scanziani E, Gobbi A, Crippa L, et al. Hyperkeratosis-associated coryneform infection in severe combined immunodeficient mice. *Lab Anim*. 1998;**32**: 330–336.
52. Schofield PN, Sundberg JP, Hoehndorf R, et al. New approaches to the representation and analysis of phenotype knowledge in human diseases and their animal models. *Brief Funct Genomics*. 2011;**10**:258–265.
53. Sellers RS. The gene or not the gene—that is the question: understanding the genetically engineered mouse phenotype. *Vet Pathol*. 2012;**49**:5–15.
54. Sellers RS, Ward JM. Toward a better understanding of mouse models of disease. *Vet Pathol*. 2012;**49**:4.
55. Shuangshoti S, Rushing EJ, Mena H, et al. Supratentorial extraventricular ependymal neoplasms: a clinicopathologic study of 32 patients. *Cancer*. 2005;**103**: 2598–2605.
56. Shultz LD, Coman DR, Bailey CL, et al. "Viable motheaten," a new allele at the motheaten locus: I. Pathology. *Am J Pathol*. 1984;**116**:179–192.
57. Sills RC, Boorman GA, Neal JE, et al. Mutations in ras genes in experimental tumours of rodents. *IARC Sci Publ*. 1999;**146**:55–86.
58. Sills RC, Hong HL, Melnick RL, et al. High frequency of codon 61 K-ras A–>T transversions in lung and Harderian gland neoplasms of B6C3F1 mice exposed to chloroprene (2-chloro-1,3-butadiene) for 2 years, and comparisons with the structurally related chemicals isoprene and 1,3–butadiene. *Carcinogenesis*. 1999;**20**:657–662.
59. Simpson EM, Linder CC, Sargent EE, et al. Genetic variation among 129 substrains and its importance for targeted mutagenesis in mice. *Nat Genet*. 1997;**16**: 19–27.
60. Smith RS, Montagutelli X, Sundberg JP. Ulcerative blepharitis in aging inbred mice. In: Mohr U, Dungworth DL, Capen CC, et al, eds. *Pathobiology of the Aging Mouse*. Washington, DC: ILSI Press; 1996:131–138.
61. Suhalim JL, Parfitt GJ, Xie Y, et al. Effect of desiccating stress on mouse meibomian gland function. *Ocul Surf*. 2014;**12**:59–68.
62. Sundberg JP, Berndt A, Sundberg BA, et al. The mouse as a model for understanding chronic diseases of aging: the histopathologic basis of aging in inbred mice. *Pathobiol Aging Age Relat Dis*. 2011;**1**.
63. Sundberg JP, Brown KS, Bates R, et al. Suppurative conjunctivitis and ulcerative blepharitis in 129/J mice. *Lab Anim Sci*. 1991;**41**:516–518.
64. Tabata N, Miyazawa M, Fujisawa R, et al. Establishment of monoclonal antiretroviral gp70 autoantibodies from MRL/lpr lupus mice and induction of glomerular gp70 deposition and pathology by transfer into non-autoimmune mice. *J Virol*. 2000;**74**:4116–4126.
65. Tanaka T, Rivenson A. Mastocytoma induced by cigarette smoke particulates: "cigarette tar." *Arch Dermatol Res*. 1986;**279**:130–135.

66. Threadgill DW, Matin A, Yee D, et al. SSLPs to map genetic differences between the 129 inbred strains and closed-colony, random-bred CD-1 mice. *Mamm Genome*. 1997;**8**:441–442.
67. Threadgill DW, Yee D, Matin A, et al. Genealogy of the 129 inbred strains: 129/SvJ is a contaminated inbred strain. *Mamm Genom*. 1997;**8**:390–393.
68. To MD, Perez-Losada J, Mao JH, et al. A functional switch from lung cancer resistance to susceptibility at the Pas1 locus in Kras2LA2 mice. *Nat Genet*. 2006;**38**:926–930.
69. Vege KD, Giannini C, Scheithauer BW. The immunophenotype of ependymomas. *Appl Immunohistochem Mol Morphol*. 2000;**8**:25–31.
70. Wancket LM, Devor-Henneman D, Ward JM. Fibro-osseous (FOL) and degenerative joint lesions in female outbred NIH Black Swiss mice. *Toxicol Pathol*. 2008;**36**:362–365.
71. Ward JM. Pulmonary pathology of the motheaten mouse. *Vet Pathol*. 1978;**15**:170–178.
72. Ward JM, Anver MR, Mahler JF, et al. Pathology of mice commonly used in genetic engineering (C57BL/6; 129; B6,129; and FVB/N). In: Ward JM, Mahler JF, Maronpot RR, et al, eds. *Pathology of Genetically Engineered Mice*. Ames, IA: Iowa State University Press; 2000:161–179.
73. Ward JM, Yoon M, Anver MR, et al. Hyalinosis and Ym1/Ym2 gene expression in the stomach and respiratory tract of 129S4/SvJae and wild-type and CYP1A2-null B6,129 mice. *Am J Pathol*. 2001;**158**:323–332.
74. Woolford L, de Lahunta A, Baiker K, et al. Ventricular and extraventricular ependymal tumors in 18 cats. *Vet Pathol*. 2013;**50**:243–251.
75. Yuan R, Peters LL, Paigen B. Mice as a mammalian model for research on the genetics of aging. *ILAR J*. 2011;**52**:4–15.